Geometric approach to the precession of compact binaries

Michael Boyle, Robert Owen, and Harald P. Pfeiffer

Phys. Rev. D **84**, 124011 — Published 2 December 2011

DOI: 10.1103/PhysRevD.84.124011

A geometric approach to the precession of compact binaries

Michael Boyle and Robert Owen
Center for Radiophysics and Space Research, Cornell University, Ithaca, New York 14853, USA

Harald P. Pfeiffer
Canadian Institute for Theoretical Astrophysics, University of Toronto, Toronto, Ontario M5S 3H8, Canada

We discuss a geometrical method to define a preferred reference frame for precessing binary systems and the gravitational waves they emit. This minimal-rotation frame is aligned with the angular-momentum axis and fixes the rotation about that axis up to a constant angle, resulting in an essentially invariant frame. Gravitational waveforms decomposed in this frame are similarly invariant under rotations of the inertial frame and exhibit relatively smoothly varying phase. By contrast, earlier prescriptions for radiation-aligned frames induce extraneous features in the gravitational-wave phase which depend on the orientation of the inertial frame, leading to fluctuations in the frequency that may compound to many gravitational-wave cycles. We explore a simplified description of post-Newtonian approximations for precessing systems using the minimal-rotation frame, and describe the construction of analytical/numerical hybrid waveforms for such systems.

I. INTRODUCTION

One of the central goals of modern numerical relativity is the accurate simulation of compact binary systems, in particular the computation of the gravitational waveforms emitted by these systems. These waveforms provide crucial input into the construction of accurate template banks necessary for detection and parameter estimation based on matched filtering [1, 2] in gravitational-wave detectors such as LIGO, Virgo, LCGT [3–6], and possible space-based detectors such as LISA [7–9]. More generally, detailed and accurate knowledge of waveforms provides a dictionary to relate measured waveforms to the specific details of the astrophysical sources that give rise to those waveforms, allowing gravitational-wave experiments to fulfill their proper role as tools for extremely high-precision astrophysics.

For such a bank of gravitational waveforms to be useful, however, it must not be restricted to an astrophysically unrealistic subset of the space of source parameters. Numerical-relativity simulations must eventually treat binary systems with a broad range of mass ratios, spin magnitudes, and spin orientations. Many of the fundamental challenges on the first two points have now been overcome.[1] However, precessing binaries remain a formidable challenge. The parameter space of precessing binaries is vastly larger than for non-precessing binaries, and its exploration is just getting underway. Furthermore, the absence of precession allows simplifying assumptions about the properties of the gravitational waveforms, greatly easing post-Newtonian comparisons and simplifying gravitational-wave data-analysis strategies.

When binary systems of black holes (or neutron stars or other compact objects) have spin angular momenta that are misaligned (with one another or with the orbital angular momentum of the pair), the plane of orbital motion inclines and precesses over time. In post-Newtonian theory, this phenomenon can be interpreted as arising from spin-orbit couplings. In fully nonlinear general relativity, these dynamical effects cannot easily be understood in gauge-unambiguous language. However, the effects of this precession can be seen unambiguously in the waveform, as modulations that trade energy content between the various spherical-harmonic modes [15–17].

These modulations present difficulties for cataloging the gravitational waveforms. In non-precessing simulations, the standard practice has been to decompose each spherical harmonic component of the waveform into a time-varying amplitude and phase. Both of these elements, in non-precessing cases, can be accurately approximated before or after merger as simple polynomials or exponentially damped polynomials, greatly simplifying their description. In precessing systems, this is no longer the case.

Aside from the complexity of fitting the precessing waveforms, there is also the concern that a precessing system does not have a preferred frame of inertial coordinates. An overall rotation of the inertial coordinates would transform the various waveform modes, modulating them in different ways. This means that comparisons between waveforms must account for a rotation between the inertial frames in which they are measured. In non-precessing cases, this difficulty is avoided by the existence of a preferred, fixed axis (the axis along which the radiation is preferentially beamed). This axis is intuitively associated with the normal to the orbital plane.

Schmidt *et al.* [18] pointed out that this preferred axis, while no longer fixed in precessing cases, nonetheless still exists and can be used to rotate the inertial spatial coordinates over time, demodulating the waveform. They suggested a method for finding that axis, as did O'Shaughnessy *et al.* [19] more recently. Essentially, the idea is to find a rotation operator at each instant in time to maximize the z component of the angular momentum

[1] See reviews [10, 11], as well as [12–14] for simulations that push the limits of large mass ratios and spins.

in the radiation.[2] The z axis of the original frame, rotated by this operator, is taken to be the preferred axis. We refer to this axis as the *radiation axis*.

We expect this insight to be important for understanding and cataloging generic gravitational waveforms. Definition of the radiation axis is the first step toward frames adapted to precessing binaries, in which the gravitational waveforms have simple structure. However, fixing the *axis* does not fix the *frame*, because of the ambiguity in rotations about the axis. From a more formal perspective, the (directed) axis being tracked lives in a two-dimensional space: the space of unit vectors in $\mathbb{R}^3$, which is topologically the two sphere S^2. However the space of available rotations, the group manifold of $SO(3)$, is topologically $\mathbb{RP}^3$, which is three dimensional. In general, no mathematically preferred method exists to infer a unique path in $\mathbb{RP}^3$ from a path in S^2; additional conditions must be imposed.

Therefore, the second step toward adapted frames is to fix this rotation about the radiation axis. References [18] and [19] address the first step by providing suitable definitions of the radiation axis, but deal with the second step only implicitly through the choice of parameterization of the rotation matrices. A rotation around the radiation axis changes the phase of each gravitational-radiation mode by an integer multiple of the rotation angle. An unsuitable choice of this angle will induce unphysical variations in the gravitational-wave phases in the adapted frame, even for vanishingly small precession, as demonstrated in Sec. IV.

The present paper addresses the question of how to fix the rotation about the radiation axis. Our construction is geometric, and the resulting *minimal-rotation frame* is invariant under rotations of the inertial coordinates in which the precessing waveforms are extracted, except for the remaining freedom of a constant overall rotation. Therefore, the approach proposed here results in an essentially unique adapted frame and in gravitational waveforms that are similarly unique. In contrast, the implementations of Refs. [18] and [19] choose the final rotation angle in a coordinate-dependent manner: working in terms of Euler angles and always setting the third Euler angle to $\gamma = 0$—by construction, this is the rotation about the z axis of the adapted frame.

The key to fixing this remaining freedom by geometric means lies in an analogy with the non-precessing binary. In the non-precessing case, there are again many coordinate frames that preserve the condition that the radiation is primarily quadrupolar with $m = \pm 2$. One could arbitrarily rotate about the z axis and preserve this condition. In practice this does not pose a problem, because it is taken as physically obvious that one would not analyze the waveform in a coordinate frame that is rotating about the z axis relative to an inertial frame. A *fixed* overall rotation about the z axis is allowed, leading to the well-known overall freedom in the waveform phase. However a time-dependent rotation about the z axis, which could cause arbitrary frequency modulation in the waveform, is rejected as unnatural.

Any frame that tracks the radiation axis of a precessing binary, on the other hand, is necessarily changing. As far as possible, we would like to carry over the non-rotating condition from the non-precessing system. In this case, we can describe the rotation of the frame by the instantaneous rotation vector $\vec{\varpi}$. Relative to an inertial frame, the time derivative of any vector stationary in the rotating frame is given by

$$\dot{\vec{v}} = \vec{\varpi} \times \vec{v} \ . \tag{1}$$

If we denote the radiation axis by a unit vector $\vec{a}$, we see that $\dot{\vec{a}} = \vec{\varpi} \times \vec{a}$. Taking the cross product of both sides of this equation with $\vec{a}$ and using the standard triple-product formula, we have

$$\vec{a} \times \dot{\vec{a}} = (\vec{a} \cdot \vec{a})\, \vec{\varpi} - (\vec{a} \cdot \vec{\varpi})\, \vec{a} \ . \tag{2}$$

Using the fact that $\vec{a}$ is unit, we can rearrange this as

$$\vec{\varpi} = \vec{a} \times \dot{\vec{a}} + (\vec{a} \cdot \vec{\varpi})\, \vec{a} \ . \tag{3}$$

Of course, the component of $\vec{\varpi}$ along $\vec{a}$ is completely undetermined by this equation; we need some other condition to fix it. Now, when $\dot{\vec{a}} = 0$, as in the non-precessing case, we recover the natural non-rotating frame when $\vec{a} \cdot \vec{\varpi} = 0$. This is the same condition imposed by Buonanno, Chen, and Vallisneri [20] in the context of post-Newtonian template waveforms (discussed further in Sec. V A below). We stress the importance of this condition more broadly—and particularly in the context of numerical relativity.

Here, we augment the methods of Schmidt *et al.* and O'Shaughnessy *et al.* with the condition that the instantaneous rotation of the frame satisfy

$$\vec{\varpi} \cdot \vec{a} = 0 \ . \tag{4}$$

Hereafter, we refer to this as the condition of *minimal rotation*, as this implies that $\vec{\varpi}$ has the smallest possible magnitude, out of the infinitely many rotation vectors consistent with the known motion of the radiation axis. It is significant that this condition on $\vec{\varpi}$ is *geometrically* meaningful, because $\vec{a}$ is—at any instant—independent of the orientation of the frame in which it is found. As we will demonstrate below, the waveform decomposed in such a frame is independent of an overall rotation, up to a constant phase.

Given a rotation $\mathbf{R}(t)$ that takes the z axis into the radiation axis ($\vec{a}(t) = \mathbf{R}(t)\, \hat{z}$), we can use Eq. (4) to find a condition on $\mathbf{R}(t)$ that holds only if it is a *minimal* rotation. Alternatively, given any rotation that takes the z axis into the radiation axis, we can easily construct

[2] More specifically, the method of Schmidt *et al.* calls for a rotation that maximizes the power in the $(\ell, m) = (2, \pm 2)$ modes. However, we show in Sec. II that this can be regarded—in some sense—as a restriction of the method of O'Shaughnessy *et al.*

another rotation that does the same while also satisfying the minimal-rotation condition. These relations are the key results of this paper.

The remainder of this paper is structured as follows: In Sec. II we summarize the algorithms for finding the radiation axis presented by Schmidt *et al.* [18] and by O'Shaughnessy *et al.* [19]. We show that the first method is essentially a restriction of the second, but point out that with slight improvements to the numerical techniques both can be used find the correct radiation axis to very high accuracy—at least for simple toy models in which the correct axis is known. In Sec. III we translate the minimal-rotation condition, Eq. (4), into a condition on the rotation operator itself, and construct a method for imposing this condition while leaving the radiation axis fixed. In Sec. IV, we compare the original algorithms to this coordinate-independent method. First, we show that the motion of the coordinate axes is essentially invariant for our implementation, while the axis motion for the original methods depends sensitively on the orientation of the inertial coordinate frame. We then demonstrate that this dependence shows up in phase the waveform modes using a simple post-Newtonian model. In Sec. V, we exhibit applications of the minimal-rotation frame, which demonstrate that the usual machinery used for non-precessing waveforms can be directly carried over to precessing systems in this frame. In particular, we discuss a framework for calculating post-Newtonian waveforms taking advantage of this simple frame, first proposed by Buonanno, Chen, and Vallisneri [20]. We then describe how to compare waveforms and construct hybrids. Finally, in Sec. VI, we close with discussion of the benefits of this method and potential applications in analytic constructions. Two appendices detail our conventions, list some crucial formulas for rotations, and repeat our main results in the language of quaternions.

II. LOCATING THE RADIATION AXIS

The gravitational waves radiated from a compact binary are typically decomposed in a spin-weighted spherical harmonic expansion of the field on a sphere. For a binary with orbital angular momentum $\vec{L}$ along the z axis, the dominant modes in this expansion are the $(\ell, m) = (2, \pm 2)$ modes. When $\vec{L}$ is not along the z axis, however, the various modes will mix, and other modes of the $\ell = 2$ component can dominate. For precessing binaries, this misalignment of the angular momentum and the z axis of an inertial frame is inevitable, complicating comparisons between simulations produced with even slightly different initial conditions. Moreover, the amplitude and phase of the modes themselves will become rapidly varying functions of time, complicating analysis of the waveforms. Both of these complications can be eliminated by decomposing the waveform in a non-inertial frame that somehow tracks the motion of the binary. Two methods to do this have been presented in the literature. We now review these, showing that they can be expressed in very similar ways, noting that both can be implemented numerically to achieve very high accuracy, and highlighting the crucial degeneracy present in both.

A. The two methods

The first algorithm, presented in Schmidt *et al.* [18], finds a frame in which the amplitudes of the $(\ell, m) = (2, \pm 2)$ modes of the gravitational-wave field are maximized. Reference [18] uses the Newman-Penrose Weyl scalar Ψ_4, though the principle is the same for any radiation field—for example, the metric perturbation h. We will use the generic symbol q to establish the method. We regard q as the quantity measured in an inertial frame, and $\hat{q}$ the function under a specified rotation.[3] Each of these can be decomposed in spin-weighted spherical harmonics [Eq. (A16)], with weights of the modes denoted $q^{\ell,m}$ and $\hat{q}^{\ell,m}$. The relation between $q^{\ell,m}$ and $\hat{q}^{\ell,m}$ is given by Eq. (A17).

The basic idea is to find a rotation $\mathbf{R}(\alpha, \beta, \gamma)$ to maximize the quantity[4]

$$\begin{aligned} Q(\alpha, \beta, \gamma) &= \sum_{m=\pm 2} \left| \hat{q}^{2,m} \right|^2 \\ &= \sum_{m=\pm 2} \left| \sum_{m'=-2}^{2} q^{2,m'} \, \mathcal{D}^{(2)}_{m',m}(-\gamma, -\beta, -\alpha) \right|^2 , \end{aligned} \tag{5}$$

where the $\mathcal{D}^{(2)}_{m',m}$ are given in terms of the Euler angles by Eq. (A12). By considering the relationship between the coordinate systems, Eq. (A15), we can see that the radiation axis is given by $\vec{a} = \mathbf{R}(\alpha, \beta, \gamma)\, \hat{z}$.

O'Shaughnessy *et al.* [19] introduced another method, which finds an axis associated with the quadrupolar part of the radiation field. They begin by defining

$$\langle L_{(a} L_{b)} \rangle = \sum_{\ell, m, m'} \bar{q}^{\ell,m'} \, \langle \ell, m' | L_{(a} L_{b)} | \ell, m \rangle \, q^{\ell,m} , \tag{6}$$

where L_a is the usual angular-momentum operator [21], and for simplicity of presentation we set $\int |q|^2 \, \mathrm{d}\Omega = 1$. The radiation axis is then defined as the dominant principal axis of this matrix—the eigenvector with the eigenvalue of largest magnitude. This problem can be solved directly with standard algebraic techniques.

---

[3] To be precise, we define $\hat{q}$ to be the function satisfying $\hat{q}(\vartheta', \varphi') = q(\vartheta, \varphi)$, for any angles related by $\mathbf{R}(0, \vartheta', \varphi') = \mathbf{R}(\alpha, \beta, \gamma)\, \mathbf{R}(0, \vartheta, \varphi)$, where each $\mathbf{R}$ is a rotation operator parameterized by the Euler angles as described in Appendix A. These conventions affect details of later results—for example, the form of Eq. (5) and its independence of γ (as opposed to α).

[4] For general systems in general orientations, relations like the usual $q^{\ell,-m} = (-1)^\ell \bar{q}^{\ell,m}$ need not hold. As a result, both terms in the sum over m are required, to avoid mixing of the $|m| \neq 2$ modes.

We find it useful to think of this method in a second way. Basic results from linear algebra show us that there exists a rotation operator $\mathbf{R}$ such that the matrix $\mathbf{R}\left\langle L_{(a}\, L_{b)}\right\rangle \mathbf{R}^{-1}$ is diagonal, and that the final column of this diagonalized matrix is the dominant principal axis. To put it another way, then, this method can be regarded as finding a rotation operator that maximizes the z-z component of the rotated matrix, in which case the radiation axis is just $\vec{a} = \mathbf{R}\,\hat{z}$.

The similarity between the two methods becomes clear when we expand this rotated matrix and take the z-z component:

$$\begin{aligned}
\left(\mathbf{R}\left\langle L_{(a}\, L_{b)}\right\rangle \mathbf{R}^{-1}\right)_{zz}&\\
&= \sum_{\ell,m,m'} \bar{q}^{\ell,m'}\ \langle \ell, m'|\mathbf{R}\, L_z\, L_z\, \mathbf{R}^{-1}|\ell, m\rangle\, q^{\ell,m}\\
&= \sum_{\ell,m,m'} \bar{\hat{q}}^{\ell,m'}\ \langle \ell, m'|L_z\, L_z\, |\ell, m\rangle\, \hat{q}^{\ell,m}\\
&= \sum_{\ell,m} m^2\, \left|\hat{q}^{\ell,m}\right|^2\ .
\end{aligned} \tag{7}$$

O'Shaughnessy *et al.* suggest the possibility of limiting the range of the sum to just $\ell = 2$. If we further limit the sum to $m = \pm 2$, we have $m^2 = 4$ times the quantity Q given in Eq. (5), and the method of [19] reduces to that of [18].

Important differences remain between the implementations possible with the two methods, however. When O'Shaughnessy *et al.* sum over all relevant m modes, they are rotating the ℓ components of the waveform, which are geometrically meaningful. Thus, the full matrix $\langle L_{(a}L_{b)}\rangle$ as they define it is a tensor and therefore obeys standard rotation rules. If we limit the sum over m modes, we have a quantity that does *not* behave properly under rotations. This difference means that $\mathbf{R}$ can be solved for algebraically in the method of O'Shaughnessy *et al.*, while the method of Schmidt *et al.* requires a more active maximization procedure.

Nonetheless, we note that the method of Schmidt *et al.*, if implemented carefully, can be made quite accurate and efficient. Because the right-hand side of Eq. (5) (and even its derivatives) can be easily expressed as a known analytic function of the angles α, β, γ, the problem is perfectly suited to numerical optimization. We find that it is very easy to implement, with the code converging to the correct radiation axis within roughly 10^{-8} rad, typically using fewer than 10 function evaluations. This method is also quite robust, requiring no initial guess for the radiation axis. The speed and accuracy of this code, then, are essentially the same as the speed and accuracy of code implementing the method of O'Shaughnessy *et al.*

B. Degeneracies

In the discussion above, we glossed over a pair of degeneracies present in both of these methods. The first is trivial: the radiation axis produced by either method is really a directionless axis, rather than the directed axis we have assumed. Roughly speaking, this means that $\vec{a}$ may be either parallel or anti-parallel to the orbital angular momentum. This degeneracy may be resolved by any convenient means, such as comparison with the coordinate angular velocity. In the following, we assume that $\vec{a}$ is chosen to lie parallel to the angular momentum or—at least—points in a consistent direction from moment to moment.

The second degeneracy, however, exhibits a significant flaw in the methods as presented: both are invariant under rotations about the radiation axis, and therefore do not fix the rotation $\vec{\varpi}(t)$ uniquely. We can see this explicitly by looking at the behavior of the modes under such a rotation:

$$\hat{q}^{\ell,m} \to \hat{q}^{\ell,m}\, \mathrm{e}^{\mathrm{i}\, m\, \gamma}\ , \tag{8}$$

where γ is the angle of the rotation. Using this in either Eq. (5) or Eq. (6), we see that the phase factor cancels out, leaving no change to the expressions. We need to impose another condition to make these problems well posed. Both Schmidt *et al.* and O'Shaughnessy *et al.* break the degeneracy by simply setting the final Euler angle of the rotation to 0. In our conventions, this means setting $\gamma = 0$ at all times. But this choice means that the rotation $\mathbf{R}(\alpha, \beta, \gamma)$ depends on the inertial frame with respect to which the Euler angles are defined. For general precessing systems, it will affect the phase of the final waveform in highly nontrivial ways, as we demonstrate in Sec. IV B.

Nonetheless, the choice of $\gamma = 0$ does make the particular problem of finding the radiation axis well posed. In the next section we take that radiation axis, and use the freedom in γ to construct a geometrically meaningful frame. This requires abandoning locality in time: while the methods of Refs. [18] and [19] can be applied for each t separately, our method will result in an ordinary differential equation for the rotation matrix.

III. MINIMIZING ROTATION

The techniques just described give us one particular rotation $\mathbf{R}_{\mathrm{ra}}(t) = \mathbf{R}\big(\alpha(t), \beta(t), 0\big)$ that aligns the inertial frame with the radiation axis. But the previously noted freedom in γ means that we can first perform a rotation $\mathbf{R}_\gamma(t)$ by an angle γ about the z axis without affecting the radiation axis. We now construct a rotation

$$\mathbf{R}(t) = \mathbf{R}_{\mathrm{ra}}(t)\, \mathbf{R}_\gamma(t)\ , \tag{9}$$

and solve for $\mathbf{R}_\gamma(t)$ such that the minimal-rotation condition, Eq. (4), is satisfied. The new rotation $\mathbf{R}(t)$ will simultaneously satisfy the minimal-rotation condition and align the inertial z axis with the radiation axis. To find $\mathbf{R}_\gamma$, we express Eq. (4) in terms of the rotation operator $\mathbf{R}$ alone, making use of generators in the Lie algebra

$\mathfrak{so}(3)$, and various relations noted in Appendix A. We then apply this to the case where $\mathbf{R}$ is decomposed as in Eq. (9), allowing us to solve for the minimal rotation.

A. The minimal-rotation condition in terms of the rotation operator

We begin by defining the equivalents of the instantaneous rotation axis $\vec{\varpi}$ and the radiation axis $\vec{a}$ using the isomorphism σ which maps 3-vectors into $\mathfrak{so}(3)$, given in a Cartesian basis by Eq. (A2). We write $\Pi = \sigma(\vec{\varpi})$ and $A = \sigma(\vec{a})$. Now, the dot product can also be defined for elements of $\mathfrak{so}(3)$ [as $-1/2$ times the trace of the product matrix; see Eq. (A4)], allowing us to rewrite the minimal-rotation condition as

$$\Pi \cdot A = 0 \; . \tag{10}$$

Here, Π is unknown, and A is time dependent. Therefore, we now translate these into expressions in terms of the rotation operator and the basis element $Z = \sigma(\hat{z})$.

The formula for A is simple. Recall from Sec. II that $\vec{a} = \mathbf{R}\,\hat{z}$. In terms of generators, this is $A = \mathbf{R}\,Z\,\mathbf{R}^{-1}$. The formula for Π can be found by considering Eq. (1), applied to *any* vector $\vec{v}$ that is stationary in the rotating frame. If we define $\vec{v}_0 := \mathbf{R}^{-1}(0)\,\vec{v}(0)$, we can write $\vec{v}(t) = \mathbf{R}(t)\,\vec{v}_0$ in the inertial frame. In $\mathfrak{so}(3)$, this is written $V = \mathbf{R}\,V_0\,\mathbf{R}^{-1}$. Then Eq. (1) becomes

$$\frac{\mathrm{d}}{\mathrm{d}t}\left(\mathbf{R}\,V_0\,\mathbf{R}^{-1}\right) = [\Pi, \mathbf{R}\,V_0\,\mathbf{R}^{-1}] \tag{11}$$

$$= [\dot{\mathbf{R}}\,\mathbf{R}^{-1}, \mathbf{R}\,V_0\,\mathbf{R}^{-1}] \; , \tag{12}$$

where the second line comes from expanding the derivative using Eq. (A6). If equality is to hold for arbitrary $\vec{v}$, we must have

$$\Pi = \dot{\mathbf{R}}\,\mathbf{R}^{-1} \; . \tag{13}$$

Now, using these expressions for A and Π in Eq. (10) and rearranging a little, we get another form of the minimal-rotation condition:

$$\left(\dot{\mathbf{R}}\,\mathbf{R}^{-1}\right) \cdot \left(\mathbf{R}\,Z\,\mathbf{R}^{-1}\right) = 0 \; . \tag{14}$$

This is precisely the minimal-rotation condition of Eq. (4) in operator form. We can simplify this expression slightly. Noting that the dot product is invariant under rotations, we apply the inverse rotation to each part of the product, obtaining

$$\left(\mathbf{R}^{-1}\,\dot{\mathbf{R}}\right) \cdot Z = 0 \; . \tag{15}$$

B. Solving for the initial rotation

To find $\mathbf{R}$ satisfying the minimal-rotation condition, we now insert Eq. (9) into Eq. (15). Assuming that $\mathbf{R}_{\mathrm{ra}}$ is known, and using $\mathbf{R}_\gamma = \exp(\gamma\,Z)$, this will give us a condition on γ. First, we calculate

$$\mathbf{R}^{-1}\,\dot{\mathbf{R}} = \mathrm{e}^{-\gamma\,Z}\,\mathbf{R}_{\mathrm{ra}}^{-1}\,\dot{\mathbf{R}}_{\mathrm{ra}}\,\mathrm{e}^{\gamma\,Z} + \dot{\gamma}\,Z \; . \tag{16}$$

Note that conjugation by $\mathrm{e}^{-\gamma\,Z}$ does not affect the component along Z. Therefore, plugging this result into Eq. (15) and rearranging, we obtain

$$\dot{\gamma} = \left(-\mathbf{R}_{\mathrm{ra}}^{-1}\,\dot{\mathbf{R}}_{\mathrm{ra}}\right) \cdot Z \; . \tag{17}$$

Because $\mathbf{R}_{\mathrm{ra}}$ is known, we can simply evaluate the right-hand side, integrate to find $\gamma(t)$, and insert this back into Eq. (9) to find a minimal-rotation operator that takes the z axis into the radiation axis.

We emphasize that the derivations of Eqs. (15) and (17) did not assume any features of $\mathbf{R}$ and $\mathbf{R}_{\mathrm{ra}}$ other than the fact that they rotate the z axis of the inertial frame into the radiation axis. In particular, we did not assume that the final Euler angle was zero—or indeed use any expression in terms of the Euler angles. Also, though inspired by the Euler angles, the definition $\mathbf{R}_\gamma := \exp(\gamma\,Z)$ is independent of coordinates on $SO(3)$.[5] Therefore, Eq. (17) is a geometrically general equation: it should hold regardless of any coordinates we might choose for $SO(3)$, and should take the same form regardless of the inertial frame we use to find the radiation axis. One result of this is the fact that frames satisfying the minimal-rotation condition are unique up to a constant overall rotation about the radiation axis, corresponding to the integration constant obtained from integrating Eq. (17). We discuss this freedom further in Sec. V B.

Nonetheless, for the purposes of implementation, an explicit formula involving the Euler angles will be useful. When $\mathbf{R}_{\mathrm{ra}}(t) = \mathbf{R}\big(\alpha(t), \beta(t), 0\big)$, a straightforward calculation using Eqs. (A7) and (A8) gives us[6]

$$\dot{\gamma} = -\dot{\alpha}\,\cos\beta \; . \tag{18}$$

Schmidt *et al.* [18] pointed out that the orbital frequency in the rotating frame given by $\mathbf{R}_{\mathrm{ra}}$ should be roughly

[5] Note the distinction between the choice of *basis* for $\mathbb{V}^3$ and the choice of *coordinates* for $SO(3)$. Here, the basis $(\hat{x}, \hat{y}, \hat{z})$ produces the canonical basis of generators (X, Y, Z) for $\mathfrak{so}(3)$ by eigenvector problems. In particular, Z represents the unique generator having eigenvector $\hat{z}$ with eigenvalue 0, and eigenvector $(\hat{x} + \mathrm{i}\,\hat{y})/\sqrt{2}$ with eigenvalue i. Also, the exponential function is defined geometrically (see Eq. (A1) or Ref. [22]), which shows that $\exp(\gamma\,Z)$ is independent of coordinates on $SO(3)$. Similarly, the arbitrary choice of z axis will not affect the form of these equations; we can choose any unit vector as the z axis, and as long as the rotation operators take that vector into the radiation axis, the expressions will not change.

[6] Near the coordinate singularities at $\beta = 0$ and $\beta = \pi$, the value of α will contain substantial numerical noise. Differentiating α, as in this equation, simply magnifies that noise. For some configurations, we find improved numerical results when integrating this equation by parts and implementing it as $\gamma = -\alpha\,\cos\beta - \int \alpha\,\dot{\beta}\,\sin\beta\,\mathrm{d}t$.

$\Omega + \dot{\alpha} \cos\beta$ (in our notation), where Ω is the magnitude of the orbital frequency measured in the non-rotating frame. Thus our adjustment to their technique can be thought of as removing that second term, so that the orbital frequency in the rotating frame given by $\mathbf{R}$ should be roughly Ω. We will return to this observation in Sec. V A to discuss a simplification of the post-Newtonian representation of precessing systems.

IV. THE EFFECTS OF ENFORCING THE MINIMAL-ROTATION CONDITION

No preferred inertial frame exists for general precessing systems. Indeed, no preferred *axis* exists for choosing an inertial frame. When the total angular momentum $\vec{J}$ points in a constant direction, this can be a useful choice of axis, but $\vec{J}$ will change direction for inspiralling precessing systems. We might therefore expect data from different numerical simulations, for example, to be presented in different inertial frames. A key concern, then, is the behavior of the rotated frame under fixed rotations of the inertial frame. We now demonstrate that a frame aligned with the radiation axis using $\gamma = 0$ behaves poorly under such rotations, whereas such a frame with the minimal-rotation condition imposed is essentially invariant. First, we observe the motion of the rotated axes in the two cases. Then, we inspect the behavior of the phase of the waveform decomposed in the rotating frames.

A. Rotation history in different inertial frames

For any rotation $\mathbf{R}(t)$, we visualize its "rotation history" by plotting the paths of the tips of the rotated basis vectors, $\hat{x}'$, $\hat{y}'$, and $\hat{z}'$, on the unit sphere. We demonstrate the rotation histories for a toy model in which the radiation axis $\vec{a}$ precesses about a fixed axis $\vec{F}$, where $\vec{a}$ is inclined to $\vec{F}$ by an angle of 25°. In the first panel of Fig. 1, we show the rotation history for this system when $\vec{F}$ is along the z axis and the final Euler angle is simply set to $\gamma = 0$. The blue circle traces the path of the radiation axis—which coincides with the $\hat{z}'$ basis vector—while the red and green curves trace the paths of the $\hat{x}'$ and $\hat{y}'$ axes, respectively.

If, instead of being aligned with the z axis of the inertial frame, the $\vec{F}$ axis is tipped, we obtain different rotation histories. Later panels of Fig. 1 show the histories when $\vec{F}$ is tilted by the given amount. In each panel, the blue curve remains the same, being simply shifted on the sphere by the given tilt. However, the paths of the other two axes of the adapted frame change drastically as the inclination of $\vec{F}$ is changed, even undergoing topological transitions as this inclination passes the 25° precession inclination and its 65° complement. The tracked frame thus has a time-dependent rotation about the radiation axis, which will show up as a time-dependent modulation of the waveform phase. This modulation is determined by the choice of inertial frame, and therefore the phase of a waveform measured in a frame obtained with $\gamma = 0$ is not invariant in any useful sense. This phase modulation will be examined directly in Sec. IV B.

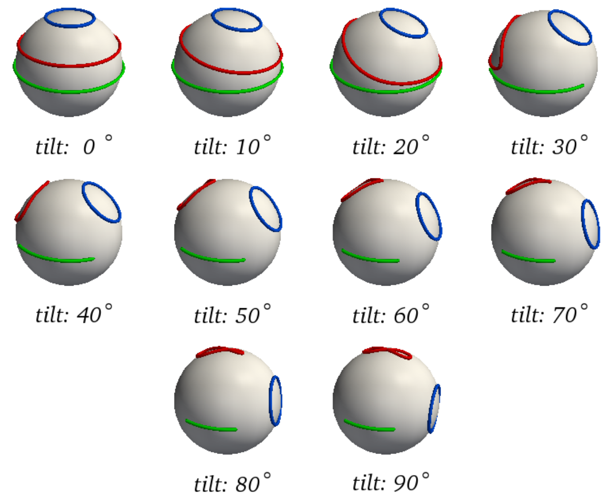

FIG. 1. Rotation histories for a simple precessing system when $\gamma = 0$. The axis denoted by the blue curve (the small, perfectly circular loop) precesses through a single cycle around a fixed axis that is tilted by varying amounts. The other axes of the tracked frame (red and green curves) take paths that depend on the inclination of the axis around which the precession occurs, relative to the inertial frame. The y axis, in particular, is forced to remain on the x-y plane of the visualization coordinates, by the choice of $\gamma = 0$. If we had defined Euler angles by z-x-z rotations, as in Ref. [18], then it would have been the x axis that was forced to remain on this plane.

We can repeat this comparison of rotation histories when the third Euler angle is set by the minimal-rotation condition, Eq. (18). The results are shown in Fig. 2. In this case, the rotation histories have the same shapes, but are simply tilted with respect to each other. That similarity shows that frames constructed with the minimal-rotation condition are essentially[7] invariant under fixed rotations of the inertial frame. As we will now see, the waveform measured in such a frame is similarly invariant.

B. Waveforms in different inertial frames

The methods set forth in Refs. [18] and [19] fix the axis of the rotated frame in an invariant way, but rely on

[7] There is still an overall freedom in a fixed rotation about the initial radiation axis. This corresponds to the standard ambiguity in orientation, which must be fixed by other methods, discussed in Sec. V B.

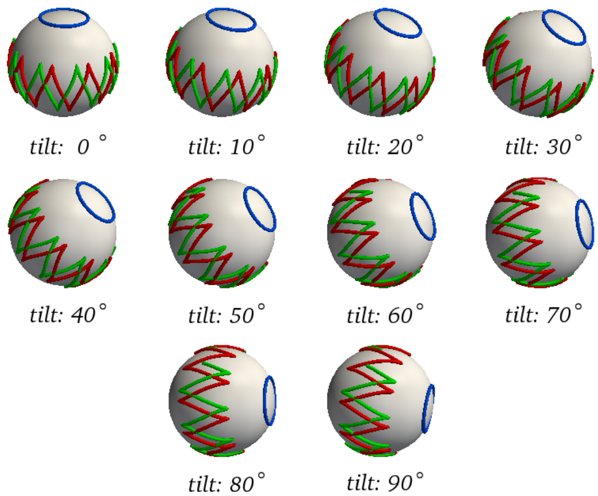

FIG. 2. Rotation histories for a simple precessing system when γ is set by Eq. (18). These systems are just the same as in Fig. 1, except that the frame is given a final rotation about the z axis to satisfy the minimal-rotation condition. The paths are identical in each case, but tilted with respect to each other. This shows that the minimally rotated frame is essentially invariant under fixed rotations of the inertial frame. Note that the paths in these figures represent many precession cycles, each corresponding to a single cycle of the "zigzag" pattern.

coordinate-degrees of freedom to fix rotations about that axis. Such a rotation translates directly into the phase of the waveform measured in the rotated frame. Since the minimal-rotation condition is imposed with a rotation about this radiation axis, only the phase of the waveform is affected. Therefore, we ignore the waveform amplitude, as it is invariant as soon as the radiation axis is fixed. We examine the waveform phase with two examples—a simple analytical example first, followed by a more realistic model.

Imagine a system with very small precession, where the radiation axis moves with constant speed along a vanishingly narrow cone centered about the z axis. Because the cone is so narrow, we might hope that the phase of the waveform q measured in the inertial frame will be close to the phase measured in the rotated frame. Assuming the radiation axis is in the x-z plane at time $t = 0$, the rotation found by the methods of Refs. [18] and [19] will be $\mathbf{R}(\dot{\alpha}\, t, \beta, 0)$, for constants $\dot{\alpha}$ and β. We can relate the modes of the waveform measured in the rotated frame $\hat{q}^{\ell,m}$ to the modes measured in the inertial frame $q^{\ell,m}$ using Eq. (A17b). If we approximate $\beta \approx 0$, then the Wigner matrices $\mathcal{D}^{(\ell)}_{m,m'}$ are nonzero only for $m = m'$, and we have

$$\hat{q}^{\ell,m} \approx q^{\ell,m}\, \mathrm{e}^{-\mathrm{i}\, m\, \dot{\alpha}\, t} \ . \tag{19a}$$

That is, the waveform acquires an additional linearly increasing phase in the rotated frame. If the complex phase of this mode is $\phi^{\ell,m}(t)$, the change in going from a non-precessing system to a system precessing with a very small opening angle is

$$\phi^{\ell,m}(t) \to \phi^{\ell,m}(t) - m\, \dot{\alpha}\, t \ . \tag{19b}$$

Note that the additional phase only depends on the number of times the system has precessed, not the size of the precession angle. If, on the other hand, we impose the minimal-rotation condition, Eq. (18) gives us $\gamma \approx -\dot{\alpha}\, t$, which cancels the additional phase, so that $\hat{q}^{\ell,m} \approx q^{\ell,m}$. In this sense, the minimal-rotation frame is much more natural.

More importantly, however, a frame with minimal rotation behaves nicely under fixed rotations of the inertial frame. For example, we take the same system as above, but tilt the inertial frame slightly so that the precession cone lies close to, but does *not* contain the z axis. In this case, the rotation will be $\mathbf{R}(\varphi, \vartheta, 0)$, where (ϑ, φ) are the usual spherical coordinates of the axis, which we can calculate by simple trigonometry. Using this result to transform the modes, we find

$$\hat{q}^{\ell,m} \approx q^{\ell,m}\, \mathrm{e}^{-\mathrm{i}\, m\ \mathrm{arccot}[\cot(\dot{\alpha}\, t) + \theta \csc(\dot{\alpha}\, t)]} \ , \tag{20a}$$

where $\dot{\alpha}$ is the same constant as above and $\theta > 1$ is a constant that depends on the particular values of the precession and the tilt angles.[8] In this case, the change to the waveform phase is bounded, but oscillatory:

$$\phi^{\ell,m}(t) \to \phi^{\ell,m}(t) - m\ \mathrm{arccot}[\cot(\dot{\alpha}\, t) + \theta \csc(\dot{\alpha}\, t)] \ . \tag{20b}$$

Thus, a slight change in the inertial frame causes a drastic change in the behavior of the waveform modes, which is associated with the topological change seen in Fig. 1 when the tilt exceeds 25°. In the minimal-rotation frame, on the other hand, the phase change in Eq. (20a) is counteracted by the adjustment to γ, and we still have $\hat{q}^{\ell,m} \approx q^{\ell,m}$.

These features also show up in systems with significant precession. We now turn to a post-Newtonian model of such a binary. The system we choose has equal-mass black holes, with spins $\chi = 0.99$ initially parallel to each other and orthogonal to the orbital angular momentum, which initially coincides with the z axis. The precession cone has an opening angle of roughly 15° initially, gradually widening to about 21°. Using the post-Newtonian

[8] In fact, this form of the equation applies for all small precession angles and tilts. If B is the tilt angle, then $\theta = B/\beta$, so $\theta = 0$ corresponds to the case where the precession cone is centered on the z axis, and Eq. (20) reduces to Eq. (19). Similarly, $0 < \theta < 1$ corresponds to a small tilt, for which the z axis is still within the precession cone. In this case, the additional phase is roughly linear, with a superposed oscillation. $\theta = 1$ corresponds to the case where the radiation axis passes through the z axis, which is the coordinate singularity of the Euler angles, meaning that the waveform phase in the $\gamma = 0$ frame is actually undefined. Finally, $\theta > 1$ corresponds to a tilt that is larger than the precession angle, so that the z axis is not enclosed in the precession cone.

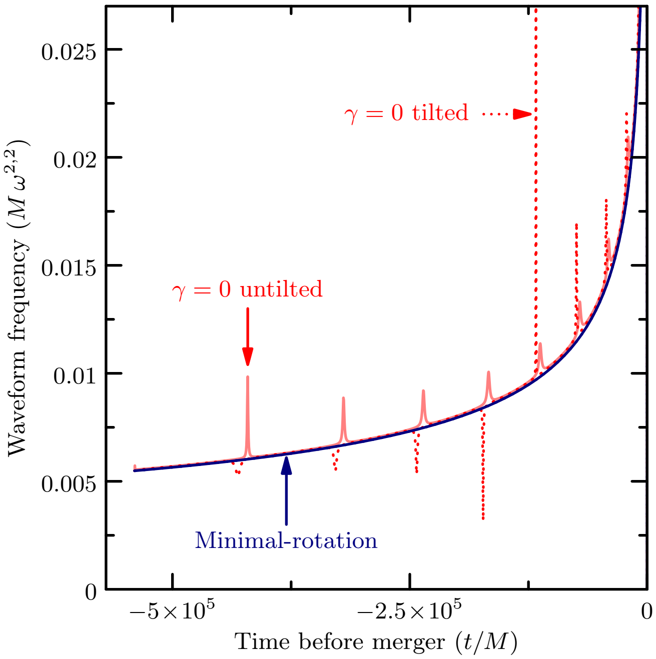

FIG. 3. Waveform frequency in various frames aligned with the radiation axis. Here, waveform frequency refers to the time derivative of the phase of the $(\ell, m) = (2, 2)$ mode of the gravitational waveform. The solid red line shows the frequency measured in a frame derived from the inertial frame by a rotation in which the third Euler angle γ is set to 0, while the solid blue line shows the same quantity in a frame for which γ satisfies the minimal-rotation condition. Clearly, the latter curve is much smoother. We also show as dotted lines the same quantities when the physical system is tilted by 10°. The dotted blue line coincides with the solid blue line, showing the invariance of the waveform in that frame.

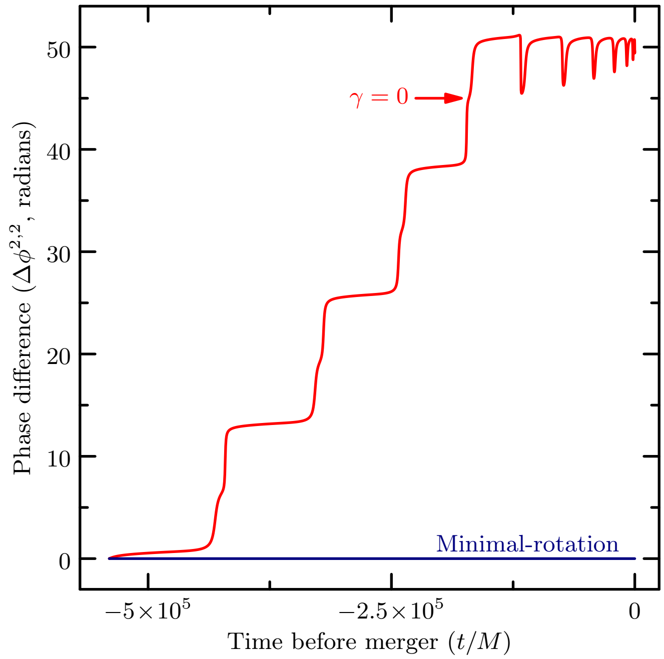

FIG. 4. Change of phase measured in frames aligned to the radiation axis when the physical system is tilted by 10°. This phase difference is defined by Eq. (21), and plotted for two cases: the first (in red) where $\phi^{2,2}$ refers to phases measured in a frame obtained from the inertial frame with a rotation in which the final Euler angle γ is set to 0; the second (in blue) where $\phi^{2,2}$ refers to phases measured in frames satisfying the minimal-rotation condition. The change in phase for the minimal-rotation frames is 0 to within numerical error (roughly a part in 10^5 here). Note that this waveform extends for roughly the length of time such a system would be in the sensitive band of Advanced LIGO if the total mass were about $10\,M_\odot$.

waveform, we can the find the radiation axis with the methods described in Sec. II, then decompose the modes of the waveform either in a frame with $\gamma = 0$ or in a frame with minimal rotation.

Again, we see the two features identified above. First, the waveform decomposed in the minimal-rotation frame appears to be smoother than the waveform decomposed in the $\gamma = 0$ frame. In particular, while the amplitudes are identical in the two frames, the phase of the $(\ell, m) = (2, 2)$ mode in the $\gamma = 0$ frame is constantly increasing relative to the phase in the minimal-rotation frame, and jumps each time the radiation axis passes near the z axis (each time $\dot{\alpha}\,\cos\beta$ is large). We plot the *frequency* of the $(2, 2)$ mode measured in the two frames in Fig. 3, where the phase jumps show up as spikes.

Second, the waveform phase in the minimal-rotation frame is invariant (up to a constant) under overall rotations of the inertial frame in which the waveform is measured—which is not the case for the $\gamma = 0$ frame. We illustrate this by tilting the post-Newtonian system by a 10° rotation about the y axis, and redoing the decomposition in the two frames. The frequencies for this rotated system are also plotted (as dotted lines) in Fig. 3, where we see that the curves for the minimal-rotation frame lie on top of each other, while the $\gamma = 0$ curve changes but still exhibits spikes.

Figure 4 plots the phase-differences of the (2,2) mode between the two post-Newtonian evolutions differing by a rotation by 10°,

$$\Delta\phi^{2,2} = \phi^{2,2}_{\text{untilted}} - \phi^{2,2}_{\text{tilted}}. \tag{21}$$

The minimal-rotation frame is invariant under this rotation, and indeed the phases are identical to within the numerical error (as measured by convergence of the integration of Eq. (18)). The coordinate-dependent choice $\gamma = 0$, however, results in phase differences of multiple gravitational-wave cycles.

While we designed this example to be a rigorous test of the frame-alignment techniques, the later stages of inspiral and merger provide an even more stringent test, as precession frequency scales with orbital velocity. The minimal-rotation condition provides an easily implemented solution to the problems presented by the $\gamma = 0$ frame.

V. FURTHER APPLICATIONS OF THE MINIMAL-ROTATION FRAME

The minimal-rotation frame aligned with the radiation axis allows us to describe gravitational waveforms from precessing binaries very nicely. The amplitude and phase are smoothly varying functions, and are invariant (up to an overall phase offset) under rotations of the inertial frame. The significance of this construction is broader than one might immediately imagine. We now discuss some of the most important uses of gravitational waveforms, and show that the minimal-rotation frame can make the necessary manipulations much simpler.

A. Post-Newtonian waveforms

Buonanno, Chen, and Vallisneri [20] proposed the construction of template waveforms for precessing binaries, expressing the metric perturbation using the minimal-rotation frame (which they simply called the "precessing frame"). Their motivation was to separate the response of a detector into two parts: one describing the intrinsic qualities of the waveform; the other describing the position and orientation of the detector.

This description differs from the more usual approach [15, 16, 23, 24] of tracking the binary's orbital parameters in a frame related to the inertial frame by a rotation taking the z axis into the Newtonian angular momentum $\hat{L}_{\mathrm{N}}$, with the final Euler angle set to $\gamma = 0$. This results in a nontrivial relationship between the orbital frequency in the inertial frame, $\Omega_{\mathrm{inertial}}$, and the orbital frequency in the instantaneous orbital plane, $\Omega_{\mathrm{orbital}}$:

$$\Omega_{\mathrm{inertial}} = \Omega_{\mathrm{orbital}} + \dot{\alpha}\,\cos\beta\ . \tag{22}$$

In such a framework, this equation must be integrated as part of the post-Newtonian system, along with the equations for the angular momentum, spins, and the usual flux and orbital energy, resulting in the motion of the binary as a function of time. This motion is then inserted into expressions for the gravitational waveform in the inertial frame. Because of the complicated motion, these expressions are necessarily even more elaborate than the standard expressions for motion in the orbital plane [23].

We can substantially simplify the analytical prescription by evolving the orbital elements in the inertial frame, but writing the waveform in terms of spin-weighted spherical harmonics in the rotating frame aligned with the angular momentum [15]. This is particularly easy if the frame satisfies the minimal-rotation condition, Eq. (4). In this case, the instantaneous rotation vector is

$$\vec{\varpi} = \hat{L}_{\mathrm{N}} \times \dot{\hat{L}}_{\mathrm{N}}\ . \tag{23}$$

Assuming that $\hat{L}_{\mathrm{N}}$ is given by the angles α and β, then as in Sec. III B we can define the rotating frame by the operator

$$\mathbf{R}\left(\alpha(t), \beta(t), -\textstyle\int \dot{\alpha}\,\cos\beta\,\mathrm{d}t\right)\ . \tag{24}$$

In such a frame, Eq. (22) becomes

$$\Omega_{\mathrm{inertial}} = \Omega_{\mathrm{orbital}}\ . \tag{25}$$

This means that the pN orbital elements can be integrated in the usual way. That is, the orbital phase Φ obtained by integrating the angular frequency is just the phase in the rotating frame. This can then be inserted into the standard expressions [23, 25–27] for the waveform modes,[9] which gives the waveform in the rotating frame. Together with the rotation operator given by Eq. (24), this describes the waveform completely. In particular, it can readily be transformed to the inertial frame using Eq. (A17).

B. Comparing waveforms and constructing hybrids

Having obtained some model waveform, one of the first things we typically do is compare the result to some other waveform. For example, we might run a numerical simulation at two different resolutions or using two different numerical codes, and compare the output waveforms to get an estimate for their accuracy. Or we might construct an analytical model, and compare it to a numerical model of the same system. And of course, numerical simulations can only describe the last portion of the inspiral of a binary system, so we frequently combine analytical and numerical waveforms into "hybrid" waveforms. In each of these cases, the first step is to ensure that the two waveforms are expressed in the same coordinate system, which is generally referred to as *alignment*.

With various simplifying assumptions, alignment boils down to setting the time offset and the relative orientation of the frames in which the waveforms are measured. For a non-precessing binary, as discussed in Sec. I, this further reduces to setting the time offset and a single rotation around the z axis. That is, one waveform is adjusted as

$$h^{\ell,m}(t) \to h^{\ell,m}(t+\Delta t)\,\mathrm{e}^{-\mathrm{i}\,m\,\Delta\Phi}\ , \tag{26}$$

for time offset Δt and phase offset $\Delta\Phi$. The criteria used to choose those offsets typically ensure that the phase and frequency of $h^{2,2}$ are the same in both waveforms at a particular instant, for example.[10]

[9] This prescription is sufficient at the level of knowledge of post-Newtonian waveforms given in the references. However, by treating the waveform as if it were determined only by instantaneous positions and velocities, it neglects contributions which may be relevant at higher orders. For example, the standard expressions for the waveform amplitudes assume accelerations are orthogonal to the orbital angular velocity, which is not the case for precessing systems. Nonetheless, these contributions can be calculated and projected into the rotating frame. As these are higher-order spinning terms, we ignore them at this level.

[10] Many other possible criteria exist for choosing these offsets (see, e.g., Ref. [28]) but the effect on the waveform should always be given by Eq. (26). Therefore we ignore the particular criteria in use.

Precession complicates this simple picture, because we can no longer rotate the second system by just one angle $\Delta\Phi$. In general, the inertial frames will be related by some rotation $\mathbf{R}_\mathrm{f}$, which rotates the second frame into the first. We would need to solve for this rotation, which might involve rotating the entire $\ell = 2$ component of the waveform to minimize some measure of the difference between the waveforms, for example. This is cumbersome, and would inherently depend on the inertial frame in which the waveforms are measured.

Alternatively, we can measure the two waveforms in minimal-rotation frames aligned with their respective radiation axes. In that case, Sec. IV B showed that, again, the only freedom to choose coordinates for the waveforms lies in the time offset Δt and a single phase offset rotating the system about the radiation axis by $\Delta\Phi$. This, of course, would *not* be the case if the frame failed to satisfy the minimal-rotation condition.

These waveforms will also come with rotations $\mathbf{R}_1(t)$ and $\mathbf{R}_2(t)$, which describe the orientation of their frames relative to some inertial frames. Again, these inertial frames need not be the same. However, if our criteria for setting the time and phase offsets make the waveforms equal at some fiducial time t_fid, we can now directly solve for their relationship:

$$\mathbf{R}_\mathrm{f} = \mathbf{R}_1^{-1}(t_\mathrm{fid})\,\mathbf{R}_2(t_\mathrm{fid}+\Delta t)\,\mathrm{e}^{\Delta\Phi\,Z} \ . \tag{27}$$

This value of $\mathbf{R}_\mathrm{f}$ is then a constant, to be used at all times. More generally, we define a new rotation operator

$$\mathbf{R}'_2(t) = \mathbf{R}_2(t+\Delta t)\,\mathbf{R}_\mathrm{f}^{-1} \ . \tag{28}$$

This operator is more directly comparable to the first rotation operator, in the sense that $\mathbf{R}_1(t_\mathrm{fid}) = \mathbf{R}'_2(t_\mathrm{fid})$.

Now, waveform comparisons for non-precessing systems typically measure differences between amplitudes and phases of the aligned waveforms. In precessing systems decomposed in the aligned frame, it makes sense to show the same quantities. However, it is now also important to examine how the frames are aligned as functions of time. The first interesting quantity to compare might be the angle between the two radiation axes, $\vec{a}_1$ and $\vec{a}'_2 = \mathbf{R}'_2\,\hat{z}$. A simple formula that expresses this angle is

$$\delta\beta \coloneqq \arccos\left[(\mathbf{R}_1\hat{z})\cdot(\mathbf{R}'_2\hat{z})\right] \ . \tag{29}$$

We also need to understand the relative rotation *about* the radiation axis, which is particularly important because it translates directly into the phase of the waveform. There is no unique way to define this phase, whenever the two radiation axes are misaligned. In analogy with the above, we might use $\arccos\left[(\mathbf{R}_1\,\hat{y})\cdot(\mathbf{R}'_2\hat{y})\right]$. However, this can be dominated by the tilt of the radiation axes, so we attempt to remove that part of the rotation. That is, we define the rotation $\mathbf{R}_{1\to 2'}$ that takes $\vec{a}_1$ into $\vec{a}'_2$ "directly" by rotating through an angle $-\delta\beta$ about the axis $\vec{a}_1\times\vec{a}'_2$. This can be conveniently calculated by the axis-angle formulation or quaternions, as described in Appendix. B. Then, the following fulfills our needs:

$$\delta\gamma \coloneqq \arccos\left[(\mathbf{R}_{1\to 2'}\,\mathbf{R}_1\,\hat{y})\cdot(\mathbf{R}'_2\hat{y})\right] \ . \tag{30}$$

These two angles are enough to characterize the misalignment of two frames.

We can also use the aligned frame to construct hybrid waveforms joining analytical and numerical waveforms in the simple manner used for non-precessing systems [29]. When hybridizing, we use information from only the first waveform before some time t_1, and information from only the second waveform after some time t_2, with some transition in between. This is typically accomplished using a transition function $\tau(t)$ that equals 1 before t_1, 0 after t_2, and transitions smoothly in between. Then, for any quantity q, such as the amplitude or phase of a particular mode, we define that quantity in the hybrid as

$$q_\mathrm{hybrid}(t) = q_1(t)\,\tau(t) + q_2(t)\,[1-\tau(t)] \ . \tag{31}$$

The same method does not apply trivially when applied to the rotation operators $\mathbf{R}_1$ and $\mathbf{R}'_2$, but we can suggest a simple method. Various techniques have been developed by researchers in computer graphics to allow interpolation of rotation operators—typically with such unfortunate names as slerp [30], nlerp, and even log-quaternion lerp [31]. Regardless of the details, any of these can be used to define the interpolant $\mathbf{R}_\mathrm{interp}(x;t)$, which equals $\mathbf{R}_1(t)$ when $x=1$ and $\mathbf{R}'_2(t)$ when $x=0$. We can then define the hybrid rotation operator as

$$\mathbf{R}_\mathrm{hybrid}(t) = \mathbf{R}_\mathrm{interp}\big(\tau(t);t\big) \ , \tag{32}$$

completing the formulation of the hybrid.

VI. DISCUSSION

A new element has now been added to the description of a gravitational waveform. The complete description consists of three elements:

1. specification of the inertial frame in which the waveform may be measured,
2. the operator $\mathbf{R}(t)$ that rotates the inertial frame into the frame in which the modes of the waveform are decomposed, and
3. the modes of the waveform as measured in this rotated frame.

The new element is item 2; previously, the waveform would simply be decomposed in the inertial frame. References [18] and [19] introduced criteria for choosing $\mathbf{R}(t)$ such that the *amplitudes* of the waveform modes become simpler. Our contribution has been the introduction of an additional criterion which simultaneously makes the choice of $\mathbf{R}(t)$ essentially unique and makes the *phases* of the waveform modes simpler. Crucially, we developed the simple formula in Eq. (18) for imposing our criterion.

This change to the description of waveforms has many benefits for precessing systems. First, the amplitude and phase of the modes will be more nearly approximated by smooth functions. This means that less storage space will be needed to describe the data from numerical simulations, which is an increasingly important problem in gravitational-wave modeling [27]. Smooth functions are also crucial to several of the assumptions underlying extrapolation of numerical waveforms to infinite extraction radius, for example [32]. In general, we expect that strong spin-spin couplings will imprint the waveform modes with some non-smoothness, but this method does at least remove the inessential coordinate-dependent features, as illustrated vividly in Figs. 3 and 4.

Second, analysis of the waveforms becomes simpler. The machinery of waveform manipulation for non-precessing systems is well developed. Analytical constructions, methods for comparing waveforms to demonstrate convergence or to measure differences from analytical systems, and hybridization techniques are all broadly understood and applied. The basic approaches, however, are not designed for precessing systems analyzed in an inertial frame; many of the simplifying assumptions break down. The strength of this reformulation to include the rotation operator is that it simplifies the waveform modes, so that we can again use techniques designed for the non-precessing case.

ACKNOWLEDGMENTS

We thank Saul Teukolsky, Larry Kidder, Geoffrey Lovelace, and Serguei Ossokine for helpful discussions, and Richard O'Shaughnessy for pointing out Ref. [20]. This project was supported in part by a grant from the Sherman Fairchild Foundation; by NSF Grants No. PHY-0969111 and No. PHY-1005426; and by NASA Grant No. NNX09AF96G. H.P. gratefully acknowledges support from the NSERC of Canada, from the Canada Research Chairs Program, and from the Canadian Institute for Advanced Research.

Appendix A: Conventions and essential formulas

We begin by briefly reviewing the formalism of rotations of $\mathbb{R}^3$ about the origin. Such rotations form a group, described by orthogonal 3×3 matrices with determinant $+1$. The group is denoted $SO(3)$, and the group operation is composition of rotations. $SO(3)$ also forms a manifold satisfying certain consistency properties—it is a Lie group [22]. The tangent space to that manifold at the point corresponding to the group's identity element is called the Lie *algebra* $\mathfrak{so}(3)$, consisting of all antisymmetric 3×3 matrices. This Lie algebra is familiar as the generators of rotations: any $R \in \mathfrak{so}(3)$ gives rise to a rotation $\mathbf{R} \in SO(3)$ via

$$\exp : R \mapsto \mathbf{R} = \sum_{k=0}^{\infty} \frac{R^k}{k!} \ . \tag{A1}$$

We also have an isomorphism between $\mathfrak{so}(3)$ (with the matrix commutator as product) and the standard 3-vectors $\mathbb{V}^3$ (with the cross product). This map is most easily represented in a standard Cartesian frame, where the vector $\vec{v} = v^k\, \vec{x}_{(k)}$ is mapped as

$$\sigma : v^k \mapsto -\epsilon^i{}_{jk}\, v^k = \begin{pmatrix} 0 & -v^z & v^y \\ v^z & 0 & -v^x \\ -v^y & v^x & 0 \end{pmatrix}^i{}_j \ . \tag{A2}$$

In particular, we will use the isomorphism relation

$$\sigma(\vec{v}\times\vec{w}) = [\sigma(\vec{v}), \sigma(\vec{w})] \ , \tag{A3}$$

for any $\vec{v}, \vec{w} \in \mathbb{V}^3$. We will also use the Cartesian basis $(\hat{x}, \hat{y}, \hat{z})$ for $\mathbb{V}^3$, corresponding to the basis (X, Y, Z) for $\mathfrak{so}(3)$. We can decompose any element of $\mathfrak{so}(3)$ in this basis by translating the dot product into $\mathfrak{so}(3)$:

$$A \cdot B \coloneqq -\frac{1}{2} \sum_{i,j} A^i{}_j\, B^j{}_i \ , \tag{A4}$$

which satisfies $\vec{a}\cdot\vec{b} = \sigma(\vec{a})\cdot\sigma(\vec{b})$. This can be useful as in Eq. (15), for example, where the component along Z must be taken.

In this context, several formulas will be very useful. For any rotation $\mathbf{R} \in SO(3)$ and vector $\vec{v} \in \mathbb{V}^3$,

$$\sigma : \mathbf{R}\,\vec{v} \mapsto \mathbf{R}\,\sigma(\vec{v})\,\mathbf{R}^{-1} \ . \tag{A5}$$

For any differentiable curve $\mathbf{R}(t) \in SO(3)$,

$$\frac{\mathrm{d}}{\mathrm{d}t}\mathbf{R}^{-1}(t) = -\mathbf{R}^{-1}(t)\,\dot{\mathbf{R}}(t)\,\mathbf{R}^{-1}(t) \ . \tag{A6}$$

If $R(t) \in \mathfrak{so}(3)$ is a curve such that $\mathbf{R}(t) = \exp R(t)$, then whenever $R(t) \neq 0$ we can calculate

$$\mathbf{R}^{-1}\,\dot{\mathbf{R}} = \dot{R} - \frac{1-\cos r}{r^2}\,[R, \dot{R}] + \frac{r - \sin r}{r^3}\,\big[R, [R, \dot{R}]\big] \ , \tag{A7}$$

where r is the magnitude of the nonzero eigenvalues of R, which also equals the vector norm $|\vec{r}| = \left|\sigma^{-1}(R)\right|$. For any t such that $R(t) = 0$, only the first term remains. Finally, for $A, B \in \mathfrak{so}(3)$ with $A \neq 0$,

$$\mathrm{e}^A\, B\, \mathrm{e}^{-A} = B + \frac{1-\cos a}{a^2}\,\big[A, [A, B]\big] + \frac{\sin a}{a}\,[A, B] \ , \tag{A8}$$

where a is similarly the magnitude of the nonzero eigenvalues of A. Obviously, when $A = 0$, only the first term remains.

Euler angles form one convenient set of coordinates for $SO(3)$. We define the Euler angles using the z-y'-z'' convention,[11] where the first rotation is through an

[11] Note that the z-x'-z'' convention is more standard in classical mechanics—as in Ref. [33], for example. The z-y'-z'' convention, however, is more standard when using spherical harmonics, as we do here.

angle α about the z axis, the second through β about the (new) y' axis, and the third through γ about the (new) z'' axis. Note that this is equivalent to rotations in the opposite order about the *fixed* set of axes z-y-z—which is an especially useful form for calculations. In particular, we can express the rotation operator as

$$\mathbf{R}(\alpha,\beta,\gamma) = \mathrm{e}^{\alpha\, Z}\, \mathrm{e}^{\beta\, Y}\, \mathrm{e}^{\gamma\, Z} \ . \tag{A9}$$

Note that, in this convention, the singularities of the Euler angle coordinates occur when $\beta = 0$ or $\beta = \pi$.

The Wigner matrices $\mathcal{D}^{(\ell)}$ form a representation of the rotation group. That is, we know that a composition of rotations in $SO(3)$ given by

$$\mathbf{R}(\alpha,\beta,\gamma) = \mathbf{R}(\alpha',\beta',\gamma')\, \mathbf{R}(\alpha'',\beta'',\gamma'') \tag{A10}$$

implies the relation

$$\mathcal{D}^{(\ell)}_{m',m}(\alpha,\beta,\gamma) = \sum_{m''} \mathcal{D}^{(\ell)}_{m',m''}(\alpha',\beta',\gamma')\, \mathcal{D}^{(\ell)}_{m'',m}(\alpha'',\beta'',\gamma'') \ . \tag{A11}$$

We can find an explicit formula for the $\mathcal{D}^{(\ell)}$ as in Ref. [34] which, in our conventions, gives

$$\begin{aligned}\mathcal{D}^{(\ell)}_{m',m}(\alpha,\beta,\gamma) &= (-1)^{\ell+m} \sqrt{\frac{(\ell+m)!(\ell-m)!}{(\ell+m')!(\ell-m')!}} \\ &\times \mathrm{e}^{\mathrm{i}(m\,\alpha+m'\,\gamma)} \sum_{\rho} (-1)^{\rho} \binom{\ell+m'}{\rho} \binom{\ell-m'}{\rho-m-m'} \\ &\times \sin\left(\frac{\beta}{2}\right)^{2\ell-2\rho+m+m'} \cos\left(\frac{\beta}{2}\right)^{2\rho-m-m'} \ . \end{aligned} \tag{A12}$$

Goldberg *et al.* [21] showed that the spin-weighted spherical harmonics [35] are simply special cases of this expression. Adopting conventions to agree with Ref. [27], we have

$${}_{s}Y_{\ell,m}(\vartheta,\varphi) = (-1)^{m} \sqrt{\frac{2\,\ell+1}{4\,\pi}}\, \mathcal{D}^{(\ell)}_{m,-s}(0,\vartheta,\varphi) \ . \tag{A13}$$

Combining Eqs. (A11) and (A13), we can immediately obtain the transformation law for the spherical harmonics under rotation of the coordinates [36]:

$${}_{s}Y_{\ell,m'}(\vartheta',\varphi') = \sum_{m} \mathcal{D}^{(\ell)}_{m',m}(\alpha,\beta,\gamma)\, {}_{s}Y_{\ell,m}(\vartheta,\varphi) \ , \tag{A14}$$

for angles satisfying

$$\mathbf{R}(0,\vartheta',\varphi') = \mathbf{R}(\alpha,\beta,\gamma)\, \mathbf{R}(0,\vartheta,\varphi) \ . \tag{A15}$$

Note that the rotation $\mathbf{R}(\alpha,\beta,\gamma)$ is uniquely fixed by this condition in a way that it would not be by simply requiring the point defined by (ϑ',φ') to rotate into the point defined by (ϑ,φ). The fact that such a condition on the coordinates would not uniquely define $\mathbf{R}(\alpha,\beta,\gamma)$ is the central problem addressed by this paper.

We decompose a function q of spin weight s as

$$q(\vartheta,\varphi) = \sum_{\ell,m} q^{\ell,m}\, {}_{s}Y_{\ell,m}(\vartheta,\varphi) \ , \tag{A16}$$

We then define the rotated function $\hat{q}$ satisfying $\hat{q}(\vartheta',\varphi') = q(\vartheta,\varphi)$, where the angles are again related by Eq. (A15). We can decompose $\hat{q}$ into spin-weighted spherical harmonics in (ϑ',φ'), and use Eq. (A14) to find the relations between the components:

$$q^{\ell,m} = \sum_{m'} \hat{q}^{\ell,m'}\, \mathcal{D}^{(\ell)}_{m',m}(\alpha,\beta,\gamma) \ , \tag{A17a}$$

or equivalently

$$\hat{q}^{\ell,m} = \sum_{m'} q^{\ell,m'}\, \mathcal{D}^{(\ell)}_{m',m}(-\gamma,-\beta,-\alpha) \ . \tag{A17b}$$

These relations are special cases of more general transformations derived by Gualtieri *et al.* [17].

Appendix B: Main results in quaternion form

Another useful parameterization of the rotation group is given by the set of unit quaternions, which are useful as an efficient numerical method for representing rotations. Here, we repeat the main results of this paper (the minimal-rotation condition and a method for imposing it) in the form of quaternions. We also express the Wigner matrices $\mathcal{D}^{(\ell)}$ as functions of a quaternion, instead of Euler angles.

Quaternions may be thought of in many ways, but the form we find convenient here is that of a scalar plus a vector. The notation we use will be $Q = q_0 + \vec{q} = (q_0, q_1, q_2, q_3)$, where q_0 is the scalar part, $\vec{q}$ is the vector part, and (q_1, q_2, q_3) are the Cartesian components of the vector. The conjugate of the quaternion is $\bar{Q} = q_0 - \vec{q}$. The distinctive feature of quaternions is their unusual multiplication rule:

$$P\,Q = (p_0\, q_0 - \vec{p}\cdot\vec{q}) + (p_0\, \vec{q} + q_0\, \vec{p} + \vec{p}\times\vec{q}) \ . \tag{B1}$$

Note that this product is associative (unlike the vector cross product) but is neither commutative nor anticommutative for general quaternions. The unit quaternions satisfy $Q\,\bar{Q} = 1$, and can be thought of as points on the unit 3-sphere. The set of all unit quaternions forms a group locally isomorphic to $SO(3)$, where rotation of a vector $\vec{v}$ by the unit quaternion Q can be expressed by

$$\vec{v}' = Q\,\vec{v}\,\bar{Q} \ . \tag{B2}$$

In fact, the quaternions provide a double cover of $SO(3)$, as can be seen above by the fact that Q and $-Q$ produce the same rotation, but this does not cause any practical problems. The relationship with the axis-angle formulation of rotations is particularly clean: for a rotation through an angle δ about an axis $\hat{w}$, the quaternion is given by $Q = \cos(\delta/2) + \sin(\delta/2)\,\hat{w}$. In any case, we may think of a general rotation $\mathbf{R}$ as being precisely equivalent to some unit quaternion. For further details, we refer to standard texts (e.g., Ref. [37]).

A calculation very similar to the derivation of Eq. (13) shows us that the instantaneous rotation vector associated to the unit quaternion R is given by

$$\vec{\varpi} = 2\,\dot{R}\,\bar{R}\ . \tag{B3}$$

If R rotates the z axis into the radiation axis, $\vec{a} = R\,\hat{z}\,\bar{R}$, then the minimal-rotation condition given by Eq. (4) can be rewritten as

$$(\dot{R}\,\hat{z}\,\bar{R})_0 = 0\ , \tag{B4}$$

where the subscript on the left-hand side takes the scalar part of the expression. This equation is equivalent to the condition on the rotation operator itself given in Eq. (15).

As before, we may impose this condition by applying an initial rotation about the z axis. Thus, if R_{ra} is any quaternion rotation that takes the z axis into the radiation axis, we define the rotation $R = R_{\mathrm{ra}}\,R_\gamma$, where R_γ is a rotation through an angle γ about the z axis. Then R satisfies the minimal-rotation condition if

$$\dot{\gamma} = 2(\dot{R}_{\mathrm{ra}}\,\hat{z}\,\bar{R}_{\mathrm{ra}})_0\ . \tag{B5}$$

Again, given the result R_{ra} of some axis-alignment method, we can evaluate the right-hand side, integrate, and construct the total rotation.

Finally, if the result is to be used to rotate modes of a waveform, we need to express the Wigner matrices in quaternion form. This is done most simply by relating the Euler angles to various components of the quaternion, and substituting the results in Eq. (A12). We find

$$\begin{aligned}\mathcal{D}^{(\ell)}_{m',m}(R) = (-2)^{m-\ell}&\sqrt{\frac{(\ell+m)!(\ell-m)!}{(\ell+m')!(\ell-m')!}}\\ &\times \left[(R\hat{z})_3 - \mathrm{i}\,(R\hat{z})_0\right]^{m+m'}\left[(R\hat{z})_1 + \mathrm{i}\,(R\hat{z})_2\right]^{m-m'}\\ &\quad\times \sum_\rho (-1)^\rho \binom{\ell+m'}{\rho}\binom{\ell-m'}{\rho-m-m'}\\ &\times \left[1-(R\hat{z}\bar{R})_3\right]^{\ell+m'-\rho}\left[1+(R\hat{z}\bar{R})_3\right]^{\rho-m-m'}\ . \end{aligned} \tag{B6}$$

This expression can be used in Eq. (A17a); for Eq. (A17b), $\bar{R} = R^{-1}$ should replace R in this expression.

[1] L. S. Finn, Phys. Rev. D **46**, 5236 (1992).
[2] L. S. Finn and D. F. Chernoff, Phys. Rev. D **47**, 2198 (1993).
[3] B. C. Barish and R. Weiss, Phys. Today **52**, 44 (1999).
[4] D. Sigg and the LIGO Scientific Collaboration, Class. Quant. Grav. **25**, 114041 (2008).
[5] F. Acernese *et al.*, Class. Quant. Grav. **25**, 184001 (2008).
[6] K. Kuroda and the LCGT Collaboration, Class. Quant. Grav. **27**, 084004 (2010).
[7] T. A. Prince, P. Binetruy, J. Centrella, L. S. Finn, C. Hogan, G. Nelemans, E. S. Phinney, B. Schutz, and LISA International Science Team, in *American Astronomical Society Meeting Abstracts*, Bulletin of the American Astronomical Society, Vol. 38 (2006) p. 990.
[8] P. L. Bender *et al.*, *LISA. Laser Interferometer Space Antenna for the detection and observation of gravitational waves*, Tech. Rep. (Max-Planck-Institut für Quantenoptik, München, Germany, 1998).
[9] O. Jennrich, Class. Quant. Grav. **26**, 153001 (2009).
[10] J. Centrella, J. G. Baker, B. J. Kelly, and J. R. van Meter, Rev. Mod. Phys. **82**, 3069 (2010).
[11] S. T. McWilliams, Class. Quant. Grav. **28**, 134001 (2011).
[12] C. O. Lousto and Y. Zlochower, Phys. Rev. Lett. **106**, 041101 (2011).
[13] G. Lovelace, M. A. Scheel, and B. Szilágyi, Phys. Rev. D **83**, 024010 (2011).
[14] G. Lovelace, M. Boyle, M. A. Scheel, and B. Szilágyi, "Accurate gravitational waveforms for binary-black-hole mergers with nearly extremal spins," (2011), arXiv:1110.2229 [gr-qc].
[15] T. A. Apostolatos, C. Cutler, G. J. Sussman, and K. S. Thorne, Phys. Rev. D **49**, 6274 (1994).
[16] L. E. Kidder, Phys. Rev. D **52**, 821 (1995).
[17] L. Gualtieri, E. Berti, V. Cardoso, and U. Sperhake, Phys. Rev. D **78**, 044024 (2008).
[18] P. Schmidt, M. Hannam, S. Husa, and P. Ajith, Phys. Rev. D **84**, 024046 (2011).
[19] R. O'Shaughnessy, B. Vaishnav, J. Healy, Z. Meeks, and D. Shoemaker, "Efficient asymptotic frame selection for binary black hole spacetimes using asymptotic radiation," (2011), arXiv:1109.5224 [gr-qc].
[20] A. Buonanno, Y. Chen, and M. Vallisneri, Phys. Rev. D **67**, 104025 (2003).
[21] J. N. Goldberg, A. J. Macfarlane, E. T. Newman, F. Rohrlich, and E. C. G. Sudarshan, J. Math. Phys. **8**, 2155 (1967).
[22] J. J. Duistermaat and J. A. C. Kolk, *Lie Groups* (Springer-Verlag, New York, NY, 1999).
[23] K. G. Arun, A. Buonanno, G. Faye, and E. Ochsner, Phys. Rev. D **79**, 104023 (2009).
[24] M. Campanelli, C. O. Lousto, H. Nakano, and Y. Zlochower, Phys. Rev. D **79**, 084010 (2009).
[25] L. Blanchet, G. Faye, B. R. Iyer, and S. Sinha, Class. Quant. Grav. **25**, 165003 (2008).
[26] C. M. Will and A. G. Wiseman, Phys. Rev. D **54**, 4813 (1996).
[27] P. Ajith, M. Boyle, D. A. Brown, S. Fairhurst, M. Hannam, I. Hinder, S. Husa, B. Krishnan, R. A. Mercer, F. Ohme, C. D. Ott, J. S. Read, L. Santamaría, and J. T. Whelan, "Data formats for numerical relativity waves," (2011), 0709.0093v3 [gr-qc].

[28] M. Boyle, Phys. Rev. D **84**, 064013 (2011).

[29] M. Boyle, D. A. Brown, and L. Pekowsky, Class. Quant. Grav. **26**, 114006 (2009).

[30] K. Shoemake, ACM SIGGRAPH Computer Graphics **19**, 245 (1985).

[31] F. S. Grassia, Journal of Graphics Tools **3**, 29 (1998).

[32] M. Boyle and A. H. Mroué, Phys. Rev. D **80**, 124045 (2009).

[33] H. Goldstein, C. P. Poole, and J. L. Safko, *Classical Mechanics*, 3rd ed. (Addison Wesley, Reading, MA, 2001).

[34] E. P. Wigner, *Group theory and its application to the quantum mechanics of atomic spectra* (Academic Press, Inc., New York, NY, 1959).

[35] E. T. Newman and R. Penrose, J. Math. Phys. **7**, 863 (1966).

[36] M. Boyle, *Accurate gravitational waveforms from binary black-hole systems*, Ph.D. thesis, California Institute of Technology (2008).

[37] C. Doran and A. Lasenby, *Geometric Algebra for Physicists* (Cambridge University Press, New York, NY, 2003).